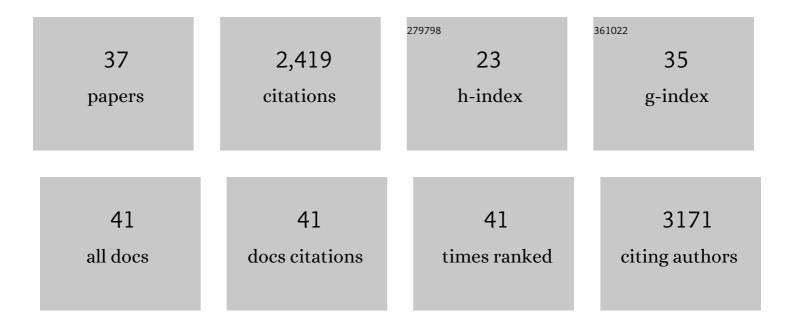
Weiqing Zheng

List of Publications by Year in descending order

Source: https://exaly.com/author-pdf/408894/publications.pdf Version: 2024-02-01



WEIDING THENC

#	Article	IF	CITATIONS
1	Higher loadings of Pt single atoms and clusters over reducible metal oxides: application to C–O bond activation. Catalysis Science and Technology, 2022, 12, 2920-2928.	4.1	7
2	Modulating the dynamics of BrÃ,nsted acid sites on PtWOx inverse catalyst. Nature Catalysis, 2022, 5, 144-153.	34.4	35
3	<i>In Situ</i> Tracking of Nonthermal Plasma Etching of ZIF-8 Films. ACS Applied Materials & Interfaces, 2022, 14, 19023-19030.	8.0	7
4	Ethane Dehydrogenation on Single and Dual Centers of Ga-modified γ-Al ₂ O ₃ . ACS Catalysis, 2021, 11, 1380-1391.	11.2	30
5	Experimental data-driven reaction network identification and uncertainty quantification of CO2-assisted ethane dehydrogenation over Ga2O3/Al2O3. Chemical Engineering Science, 2021, 237, 116534.	3.8	12
6	Polyethylene Hydrogenolysis at Mild Conditions over Ruthenium on Tungstated Zirconia. Jacs Au, 2021, 1, 1422-1434.	7.9	95
7	Intensified microwave-assisted heterogeneous catalytic reactors for sustainable chemical manufacturing. Chemical Engineering Journal, 2021, 420, 130476.	12.7	24
8	Production of renewable oleo-furan surfactants by cross-ketonization of biomass-derived furoic acid and fatty acids. Catalysis Science and Technology, 2021, 11, 2762-2769.	4.1	13
9	CO ₂ -assisted ethane oxidative dehydrogenation over MoO _{<i>x</i>} catalysts supported on reducible CeO ₂ –TiO ₂ . Catalysis Science and Technology, 2021, 11, 5791-5801.	4.1	11
10	ZnO nanorod arrays assembled on activated carbon fibers for photocatalytic degradation: Characteristics and synergistic effects. Chemosphere, 2020, 261, 127731.	8.2	26
11	Reversible Formation of Silanol Groups in Two-Dimensional Siliceous Nanomaterials under Mild Hydrothermal Conditions. Journal of Physical Chemistry C, 2020, 124, 18045-18053.	3.1	7
12	C–O bond activation using ultralow loading of noble metal catalysts on moderately reducible oxides. Nature Catalysis, 2020, 3, 446-453.	34.4	131
13	Production of high-yield short-chain oligomers from cellulose <i>via</i> selective hydrolysis in molten salt hydrates and separation. Green Chemistry, 2019, 21, 5030-5038.	9.0	32
14	Molybdenum Oxide-Modified Iridium Catalysts for Selective Production of Renewable Oils for Jet and Diesel Fuels and Lubricants. ACS Catalysis, 2019, 9, 7679-7689.	11.2	39
15	110th Anniversary: Kinetics and X-ray Absorption Spectroscopy in Methane Total Oxidation over Alumina-Supported Pt, Pd, and Ag–Pd Catalysts. Industrial & Engineering Chemistry Research, 2019, 58, 17718-17726.	3.7	8
16	Volcano curves for homologous series reactions: Oxidation of small alkanes. Applied Catalysis A: General, 2019, 587, 117255.	4.3	2
17	Molten Salt Hydrates in the Synthesis of TiO ₂ Flakes. ACS Omega, 2019, 4, 21302-21310.	3.5	4
18	Selective Hydrodeoxygenation of Vegetable Oils and Waste Cooking Oils to Green Diesel Using a Silica‧upported Ir–ReO _{<i>x</i>} Bimetallic Catalyst. ChemSusChem, 2018, 11, 1446-1454.	6.8	66

WEIQING ZHENG

#	Article	IF	CITATIONS
19	Nonâ€oxidative Coupling of Methane to Ethylene Using Mo ₂ C/[B]ZSMâ€5. ChemPhysChem, 2018, 19, 504-511.	2.1	38
20	Spectroscopic characterization of a highly selective NiCu ₃ /C hydrodeoxygenation catalyst. Catalysis Science and Technology, 2018, 8, 6100-6108.	4.1	9
21	Process Intensification for Cellulosic Biorefineries. ChemSusChem, 2017, 10, 2566-2572.	6.8	32
22	Solventless C–C Coupling of Low Carbon Furanics to High Carbon Fuel Precursors Using an Improved Graphene Oxide Carbocatalyst. ACS Catalysis, 2017, 7, 3905-3915.	11.2	72
23	Durable and self-hydrating tungsten carbide-based composite polymer electrolyte membrane fuel cells. Nature Communications, 2017, 8, 418.	12.8	42
24	Catalytic Hydrodeoxygenation of High Carbon Furylmethanes to Renewable Jetâ€fuel Ranged Alkanes over a Rheniumâ€Modified Iridium Catalyst. ChemSusChem, 2017, 10, 3225-3234.	6.8	54
25	Catalytic Hydrodeoxygenation of High Carbon Furylmethanes to Renewable Jet-fuel Ranged Alkanes over a Rhenium-Modified Iridium Catalyst. ChemSusChem, 2017, 10, 3164-3164.	6.8	0
26	Molecular structure, morphology and growth mechanisms and rates of 5-hydroxymethyl furfural (HMF) derived humins. Green Chemistry, 2016, 18, 1983-1993.	9.0	276
27	Cellulose Hydrolysis in Acidified LiBr Molten Salt Hydrate Media. Industrial & Engineering Chemistry Research, 2015, 54, 5226-5236.	3.7	63
28	The Role of Ru and RuO ₂ in the Catalytic Transfer Hydrogenation of 5â€Hydroxymethylfurfural for the Production of 2,5â€Đimethylfuran. ChemCatChem, 2014, 6, 848-856.	3.7	136
29	Vapor phase hydrodeoxygenation of furfural to 2-methylfuran on molybdenum carbide catalysts. Catalysis Science and Technology, 2014, 4, 2340.	4.1	132
30	Production of Dimethylfuran from Hydroxymethylfurfural through Catalytic Transfer Hydrogenation with Ruthenium Supported on Carbon. ChemSusChem, 2013, 6, 1158-1162.	6.8	247
31	Core–Shell Nanocatalyst Design by Combining Highâ€Throughput Experiments and Firstâ€Principles Simulations. ChemCatChem, 2013, 5, 3712-3718.	3.7	8
32	Experimental and Theoretical Investigation of Molybdenum Carbide and Nitride as Catalysts for Ammonia Decomposition. Journal of the American Chemical Society, 2013, 135, 3458-3464.	13.7	216
33	Structure–Function Correlations for Ru/CNT in the Catalytic Decomposition of Ammonia. ChemSusChem, 2010, 3, 226-230.	6.8	82
34	Effects of CeO2 addition on Ni/Al2O3 catalysts for the reaction of ammonia decomposition to hydrogen. Applied Catalysis B: Environmental, 2008, 80, 98-105.	20.2	169
35	Individual Feâ^'Co Alloy Nanoparticles on Carbon Nanotubes: Structural and Catalytic Properties. Nano Letters, 2008, 8, 2738-2743.	9.1	200
36	NH3 Decomposition Kinetics on Supported Ru Clusters: Morphology and Particle Size Effect. Catalysis Letters, 2007, 119, 311-318.	2.6	94

#	Article	IF	CITATIONS
37	Selective Hydrodeoxygenation of Vegetable Oils and Waste Cooking Oils to Green Diesel Using a Silica-Supported Ir-ReO _{<i>x</i>} Bimetallic Catalyst. ChemSusChem, 0, , .	6.8	Ο